Hindawi Publishing Corporation
Journal of Nanotechnology
Volume 2014, Article ID 321571, 8 pages
http://dx.doi.org/10.1155/2014/321571

Research Article

Growth of CuS Nanostructures by Hydrothermal Route and Its Optical Properties

Murugan Saranya, Chella Santhosh, Rajendran Ramachandran, and Andrews Nirmala Grace

Centre for Nanotechnology Research, VIT University, Vellore, Tamil Nadu 632 014, India

Correspondence should be addressed to Andrews Nirmala Grace; anirmalagladys@gmail.com

Received 27 July 2013; Revised 28 October 2013; Accepted 9 December 2013; Published 30 January 2014

Academic Editor: Jeffery L. Coffer

CuS nanostructures have been successfully synthesized by hydrothermal route using copper nitrate and sodium thiosulphate as copper and sulfur precursors. Investigations were done to probe the effect of cationic surfactant, namely, Cetyltrimethylammonium bromide (CTAB) on the morphology of the products. A further study has been done to know the effect of reaction time on the morphology of CuS nanostructures. The FE-SEM results showed that the CuS products synthesized in CTAB were hexagonal plates and the samples prepared without CTAB were nanoplate like morphology of sizes about 40–80 nm. Presence of nanoplate-like structure of size about 40–80 nm was observed for the sample without CTAB. The synthesized CuS nanostructures were characterized by X-ray diffraction (XRD), FE-SEM, DRS-UV-Vis spectroscopy, and FT-IR spectroscopy. A possible growth mechanism has been elucidated for the growth of CuS nanostructures.

1. Introduction

Semiconductor nanomaterials have attracted great interest because of their novel properties, like surface-to-volume ratio and the three-dimensional confinement of electrons, being different from those of their bulk counterparts [1–3]. In recent years, there has been an increasing interest in transition metal chalcogenides due to their novel physical and chemical properties. Covellite copper sulfide, as a member of the chalcogenides, has been used in photo thermal conversion [4], electrodes [5], nonlinear optical materials, solar controller, solar radiation absorber [6], catalyst [7], nanometer-scale switches and high-capacity cathode material in lithium secondary batteries [8], and sensors [9]. It has been observed that sulfides in nanoscale also function as photocatalyst with preferable catalytic ability [10]. Recently, various morphologies of copper sulfide including nanowires [11], nanodisks [12], hollow spheres [13], and flower-like structures [14] were prepared by thermolysis [15], microemulsion [16], hydrothermal [17, 18], solvothermal [19, 20], and polyol route [21], one-step solid-state reaction [22], chemical vapor deposition (CVD) [23], wet chemical method [24], and template-assisted [25] and sonochemical methods [26] which have been reported. Among them, the hydrothermal method is the most common synthesis technology, because of its ease of operation with less-expensive equipment. Recently, many efforts have been devoted to the synthesis of CuS nanostructures by solvothermal process at 140°C [27]. Many literatures are reported on the synthesis of CuS flakes by hydrothermal and sonochemical methods [28, 29]. CuS hexagonal nanoplates have been obtained through a vacuum chemical vapor reaction process at about 450°C [30]. Hexagonal CuS nanoplatelets have been prepared through an improved solvothermal process at 120°C [31]. CuS nanodisks have been prepared by means of solution-phase-arrested precipitation of copper sulfide nanocrystals at 182°C. In our previous work, the growth of CuS nanostructures was prepared under hydrothermal conditions at 150°C without the use of any surfactant and the effect of reaction time is reported [17].

In this work, copper sulfide nanostructures with interesting morphologies were successfully synthesized in the presence of CTAB surfactant by a simple cost-effective hydrothermal technique using water as a solvent. Use of surfactant played an important role in determining the CuS morphology and renders the stability of the nanomaterials.

Copper nitrate and sodium thiosulphate are used as copper and sulfur sources with CTAB as surfactant at 150°C for 5 and 24 hrs, respectively. The effect of reaction time and its growth mechanism has been discussed in detail. The as-prepared hexagonal nanoplate-like CuS nanostructures have excellent optical properties; the UV-Vis diffuse reflectance spectra (DRS) of the CuS nanostructure show strong and broad absorption spectra between 400 and 800 nm.

2. Materials and Methods

2.1. Materials. Copper nitrate trihydrate $Cu(NO_3)_2{\cdot}3H_2O$, sodium thiosulphate ($Na_2S_2O_3{\cdot}5H_2O$), and Cetyltrimethylammonium bromide (CTAB) were purchased from SD-Fine Chemicals, India, and they were all of analytical grade and used as received. All the samples were prepared using Milli-Q water.

2.2. Synthesis of CuS Nanomaterials. In a typical synthesis, copper nitrate trihydrate $Cu(NO_3)_2{\cdot}3H_2O$ (1 mmol) was dissolved in 40 mL of water. A green color solution was formed and 2.5 mmol of sodium thiosulphate and 0.2 mmol of CTAB were added to the above solution under vigorous stirring to ensure well dispersion of the reactants. A pale white color solution was formed, which was then transferred into a 300 mL Teflon-lined autoclave. The autoclave was then sealed and maintained at 150°C for the reaction time of 5 hrs and 24 hrs. After the reaction time, the resulting solutions were allowed to cool down at room temperature naturally. The resulting product was collected, washed several times with water and absolute ethanol, and dried under vacuum at 60°C to obtain the final product. To know the effect of CTAB, the same reaction was repeated in the absence of CTAB.

2.3. Characterization. The phase and the crystallographic structure were identified by X-ray diffraction (XRD, Philips X′ Pert Pro, Cu-Kα: $\lambda = 0.1540598$ nm). The particle size and morphology of the products were studied by FE-Scanning Electron Microscopy (FE-SEM) (HITACHI SU6600 SEM). Optical property of CuS nanostructures was done by DRS UV-Vis spectrophotometer (HITACHI U-2800). FT-IR spectra were recorded for studying the functional groups using KBr disks on a Shimadzu affinity spectrophotometer.

3. Results and Discussion

3.1. XRD Analysis. The phase composition and the phase structure of the products were examined by powder XRD. The XRD pattern of CuS nanostructures at two different reaction times (5 hrs and 24 hrs) is shown in Figure 1. From the XRD pattern, it can be seen that the resultant product is of pure phase. For all the final products at different reaction parameters, the formation of the pure covellite of CuS with hexagonal phase has been confirmed with the JCPDS data. All diffraction peaks were closely indexed with the standard peaks of CuS hexagonal phase with JCPDS card number 06-0464 and the cell parameters are $a = 3.792$ Å and $c = 16.344$ Å. No other impurity peaks were observed. The diffraction peaks are much broader than the standard peaks showing the formation of crystallites with smaller size.

As seen in the figure, the peaks are strong and sharper for a longer reaction time period of 24 hrs suggesting that the as-obtained products are well crystalline and smaller in size. This could be due to the rate of nucleation increasing at longer time periods, till it attains a well-defined stable structure. The XRD graph clearly shows peak at (100), (101), (102), (103) (008), (110), (108), and (116) as in accordance with the JCPDS file (06-0464) indicating that CuS exists as covellite phase. These peaks are in well agreement with other reports [32]. The crystalline size of CuS nanomaterials was calculated by using Scherrer's formula as follows:

$$d = \frac{k\lambda}{\beta \cos\theta}, \tag{1}$$

where "d" is the mean crystalline dimension, "k" is the crystallite shape constant (0.9), "λ" denotes the wavelength of the X-rays (Cu Kα: 1.5406 A), "β" is the full width at half maximum (FWHM) of the peak in radians, and "θ" is the diffraction angle, respectively. The average grain size was found to be 20, 24, and 22 nm for 5 hrs without CTAB, with CTAB for 5 hrs, and with CTAB for 24 hrs, respectively.

3.2. Morphological Characterization. The morphology of CuS nanostructures was investigated by FE-SEM analysis. Figures 2–4 show the FE-SEM images of CuS nanostructures prepared at 150°C for different reaction times. The reaction was also done without the presence of CTAB to know the morphology of the products. Figure 2 shows the corresponding FE-SEM images of CuS nanostructure without CTAB at different magnifications. From the figure, it can be seen that the structures were not uniform and well defined.

Figure 3 shows the SEM image of CuS nanostructures at 150°C for 5 hrs, which shows that there was not much regularity in the features. A close magnification shows the presence of nanoplates which had a mean plane size of 40–80 nm (measured edge to edge). At 5 hrs reaction time, the primary nucleation process is hindered, which allows them to aggregate to form CuS spheres, which led to the formation of irregular plate-like architectures. When compared to CuS nanostructures without CTAB, Figure 3 shows that some uniformity in stacking of nanoplates was achieved in the presence of CTAB as surfactant indicating the capping behavior of CTAB molecules to CuS crystallographic faces.

Figure 4 shows the SEM image of CuS nanostructures at 150°C for 24 hrs at various magnifications. It can be clearly seen from the figure that the structures are self-assembled to form hexagonal nanoplates. The Van der Waals force was raised due to the end-to-end growth of small platelets in CuS, which helped to form the CuS architectures. The increasing reaction time will strengthen the end to end growth and formation of hexagonal nanoplate intrinsic anisotropic CuS structure.

3.2.1. Reaction Mechanism. In this reaction process, surfactant and reaction time play a major factor influencing the morphology of the products. The addition of CTAB plays an

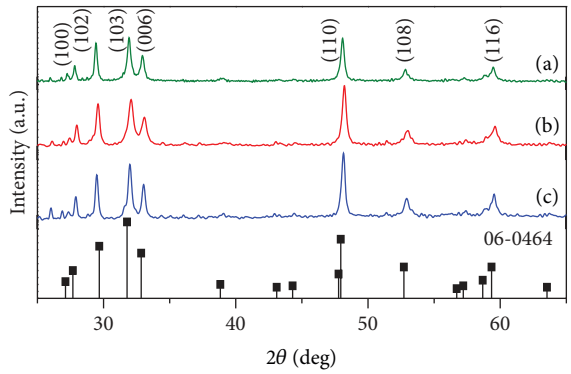

Figure 1: XRD patterns of CuS nanostructures (a) without CTAB for 5 hrs, (b) with CTAB for 5 hrs, and (c) with CTAB for 24 hrs.

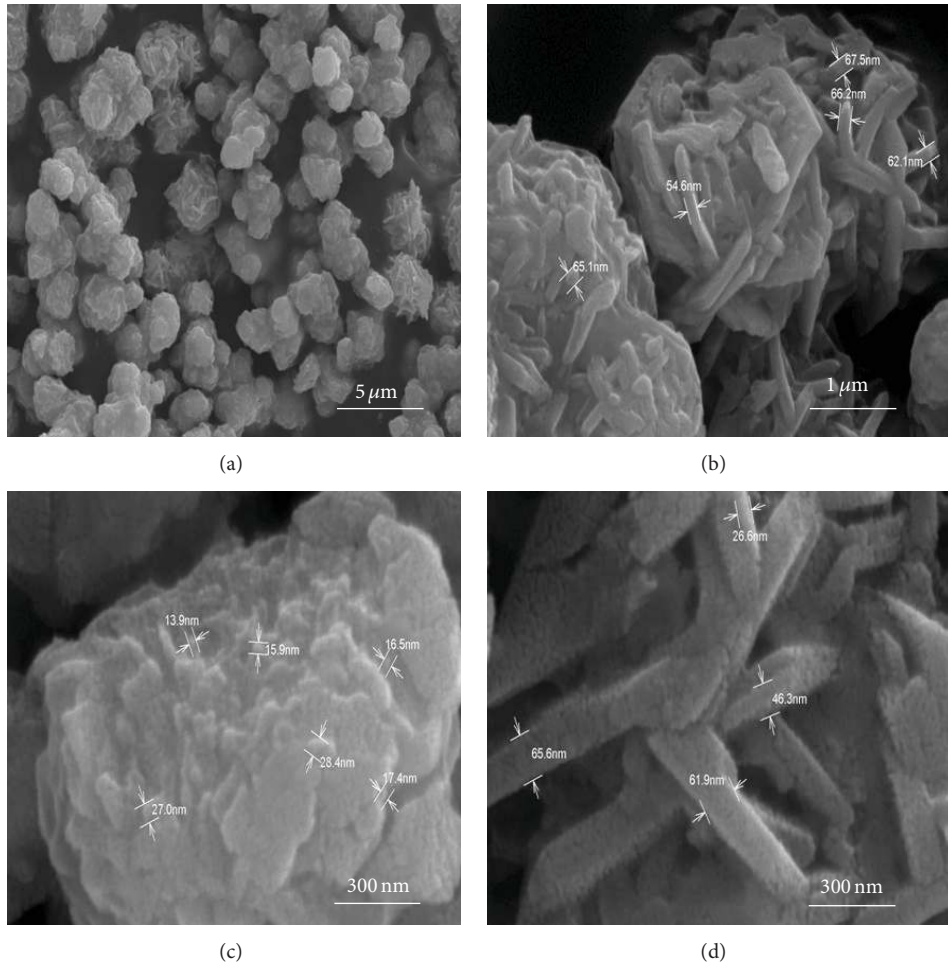

Figure 2: FE-SEM images of CuS nanostructures without CTAB for 5 hrs at 150°C at different magnifications.

important role in the formation of CuS hexagonal plates-like structure [33]. In addition, blank experiments were carried out without CTAB surfactant, where the obtained products are of irregular plate-like architectures. Hence, due to the CTAB adsorption at 150°C, the primary nucleation process is hindered, which allows them to aggregate to form CuS spheres, which will further grow preferentially along the certain face to flake-like spheres. Generally the primary aggregation is accepted. It is well known that the formation of CuS nanosheets involves 2 steps: nucleation and growth. In the nucleating stage, the plate-like seeds are formed due to the intrinsic anisotropic characteristics. Subsequently, the seeds grew along the different planes during the growth process. The hexagonal plate-like CuS consists of the alternating layers

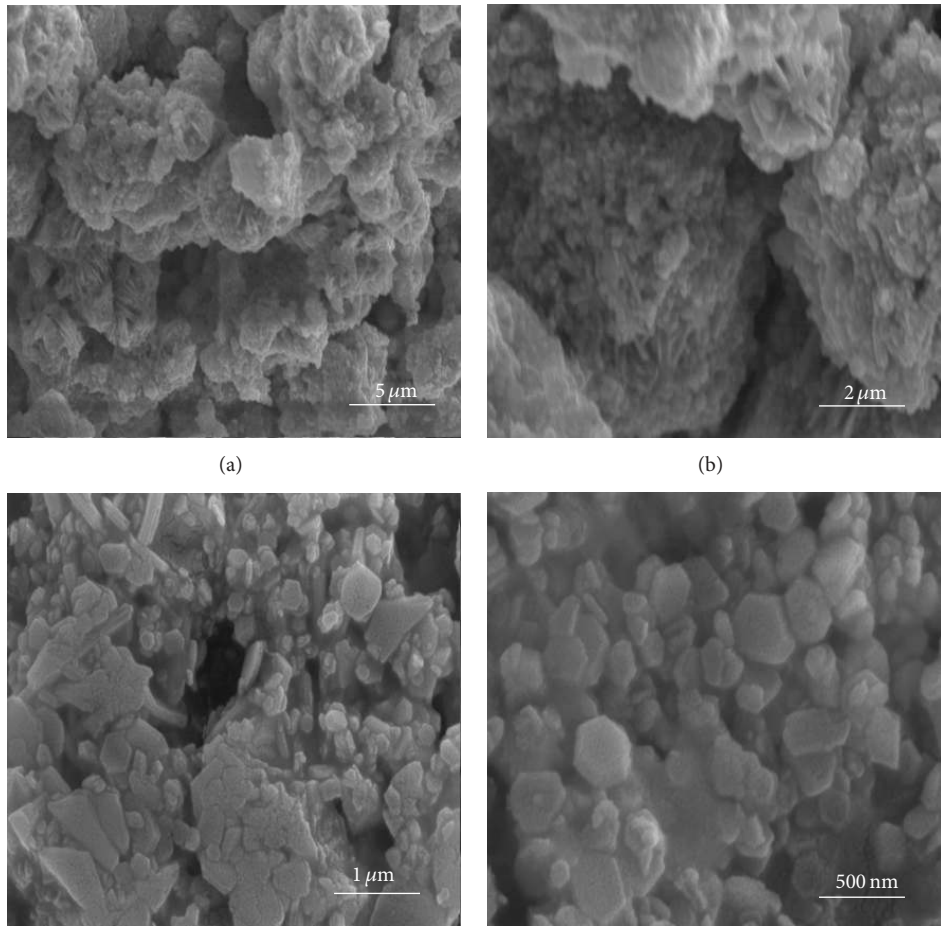

Figure 3: FE-SEM images of CuS nanostructures with CTAB at 150°C for 5 hrs at different magnifications.

with composites of CuS and Cu_2S_2. Between the layers, there exists a weak Van der Waals force that the crystal can easily cleave and obtain the smooth surfaces [34]. Hence, CuS grows like flake-type spheres. These flake-like platelets self-assemble to form CuS nanostructures. It is supposed that the nanoplates are obtained through seed-mediated growth in the presence of CTAB surfactant, which is selectively adsorbed on the various planes of CuS seed and stabilizes the formed nanoplates. The sizes of the hexagonal plates are measured to be 40–80 nm. The formation of hexagonal nanoplates might be partly related to intrinsic anisotropic structural characteristic of CuS. Simultaneously, the surfactant prevents the aggregation of the spheres and the layer reaction time promotes the flake-like nanoplates, self-assembled to form the nanostructures:

$$\begin{aligned} Cu^{2+} + {S_2O_3}^{2-} + 2H_2O &\longrightarrow [Cu(S_2O_3)(H_2O)_2] \\ Cu^{2+} + 2{S_2O_3}^{2-} &\longrightarrow [Cu(S_2O_3)_2]^{2-} \\ [Cu(S_2O_3)(H_2O)_2] &\longrightarrow CuS\downarrow + {SO_4}^{2-} + 2H^+ + H_2O \\ [Cu(S_2O_3)_2]^{2-} + 6H_2O &\longrightarrow CuS + 3{SO_4}^{2-} + 12H^+ \end{aligned} \quad (2)$$

The Cu^{2+} combine with ${S_2O_3}^{2-}$ to form $[Cu(S_2O_3)\cdot(H_2O)_2]$ and $[Cu(S_2O_3)_2]^{2-}$ in water at room temperature. This complex dissociates to supply the Cu ions and the Cu^{2+} ions combine with S^{2-} produced from the hydrolysis to form CuS. From the different reaction time the CuS nanostructures need a longer reaction time of 24 hrs rather than 5 hrs.

3.3. Optical Property of CuS Nanoplates. Figure 5 shows the UV-Vis absorption spectra of the resulting CuS products. The optical absorption spectrum of CuS materials is shown in the figure [8]. From the UV-vis figure, it shows that the samples absorb in the spectral region between 400 to 800 nm. In addition, a broad band extending into the near-IR region can be observed, which is characteristic for covellite CuS. There is a broad shoulder around 620 nm near-IR regions; that is, longer wavelength is due to free-carrier absorption. The obtained UV-Vis spectrum is slightly blue-shifted due to quantum confinement effect of CuS nanomaterial [35] as compared to the bulk CuS material [36]. For CuS nanoparticles, the wavelength increases with decreasing the particle size due to the surface scattering of free carriers. It can be concluded that the CuS nanomaterials have a broad

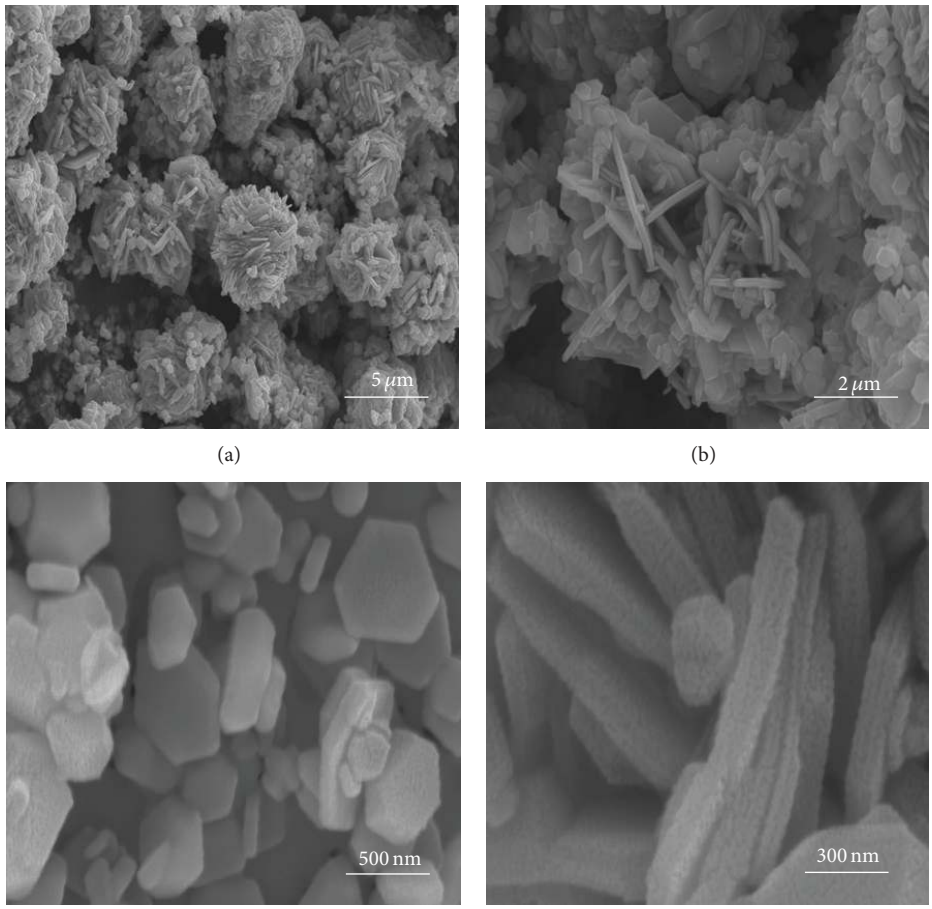

Figure 4: FE-SEM images of CuS nanostructures with CTAB at 150°C for 24 hrs at different magnifications.

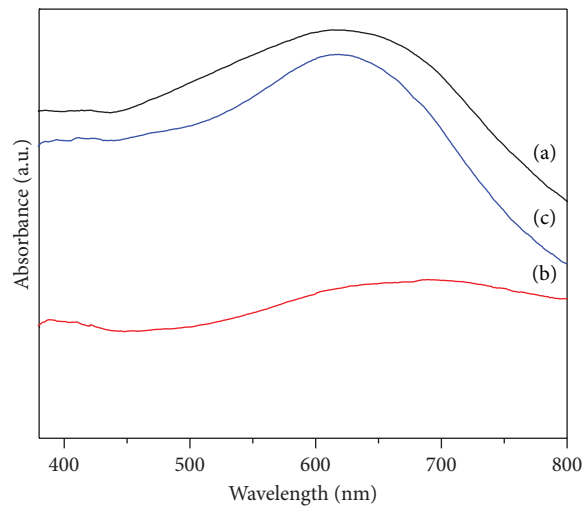

Figure 5: UV-Vis absorption spectrum of CuS nanostructures synthesized at 150°C for different reaction time (a) without CTAB 5 hrs (b) with CTAB 5 hrs (c) with CTAB 24 hrs.

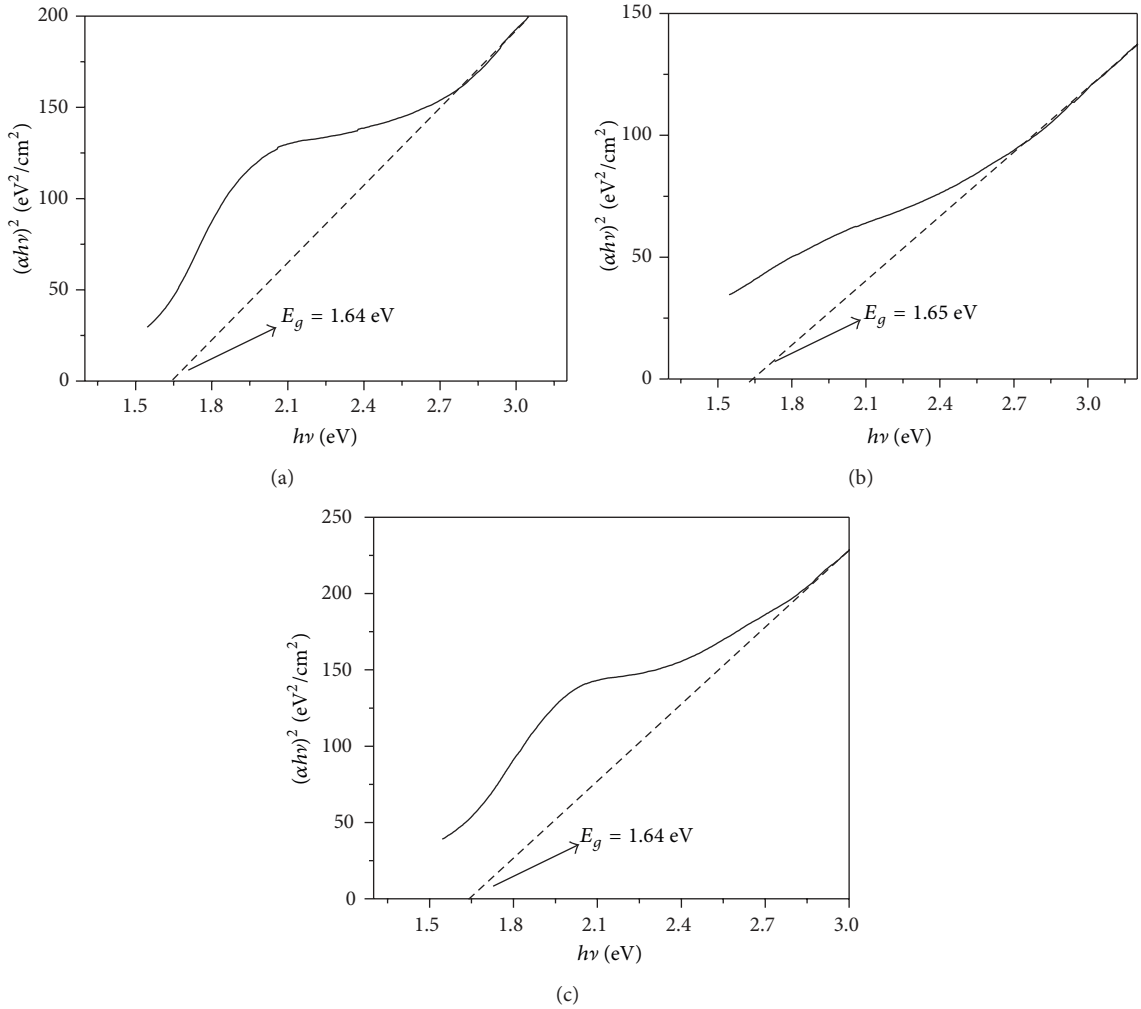

Figure 6: Optical band gap spectrum of CuS nanostructures synthesized at 150°C (a) without CTAB for 5 hrs, (b) with CTAB for 5 hrs, and (c) with CTAB for 24 hrs.

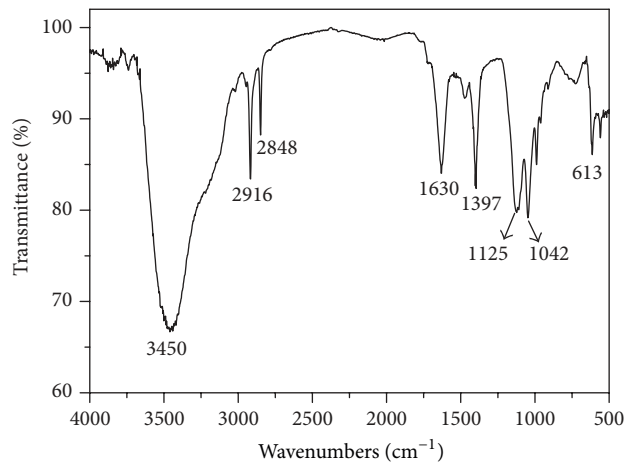

Figure 7: FT-IR spectrum of CuS nanostructures synthesized by CTAB at 150°C for 24 hrs.

absorption spectrum in both visible and near-IR regions. Thus, CuS is a promising material in the field of photocatalysis and solar cells.

From the UV-Vis figure, it is shown that the samples absorb in the spectral region between 400 and 800 nm. In addition, a broad band extending into the near-IR region can be observed, which is characteristic for covellite CuS. The optical band gap is obtained by the following equation, with the help of absorption spectra [37]:

$$(\alpha h\nu)^n = A\left(h\nu - E_g\right). \quad (3)$$

To determine the energy band gap, $(\alpha h\nu)^2$ versus $(h\nu)$ was plotted, where "α" is the absorption coefficient, "$h\nu$" is the photon energy, "A" is a constant, "E_g" is the band gap, and "n" is either 1/2 for an indirect transition or 2 for a direct transition [38]. Thus, a plot of $(\alpha h\nu)^2$ versus $(h\nu)$ is a straight line whose intercept on the energy axis gives the energy gap. According to the above equation, based on the direct transition as shown in Figure 6, the band gaps of as-obtained CuS are 1.64 eV, 1.65 eV, and 1.64 eV without CTAB for 5 hrs, with CTAB for 5 hrs, and with CTAB for 24 hrs, respectively. The obtained band gap is almost the same for all the three samples.

The FT-IR spectrum of as-prepared CuS catalyst is shown in Figure 7. The broad absorption peak around 3450 cm^{-1} corresponds to the stretching mode of the hydroxyl ions and 1630 cm^{-1} corresponds to the bending modes of H–O–H moieties of absorbed water, which indicates that the existing water molecules are absorbed by sulfide products. The presence of vibrational peak around 613 cm^{-1} indicates the presence of Cu–S stretching modes [39].

4. Conclusions

The CuS nanostructures were prepared by hydrothermal method by using copper nitrate as a copper source and sodium thiosulphate as a sulfur source in the presence of CTAB as surfactant at 150°C. The reaction was probed at two different time periods, namely, 5 hrs and 24 hrs, respectively, to know the change in the morphology of the products. X-ray diffraction pattern suggests that the CuS crystals are of pure hexagonal phase. The morphology of the products and the effect of the reaction time have been studied by using FE-SEM. It is found that CTAB plays an important role in the formation of hexagonal nanoplates. The optical property of the prepared CuS nanostructures has been studied.

Conflict of Interests

The authors declare that there is no conflict of interests regarding the publication of this paper.

Acknowledgment

The authors acknowledge the financial support of VIT University, Vellore, for supporting this work under the research associate fellowship.

References

[1] A. P. Alivisatos, "Semiconductor clusters, nanocrystals, and quantum dots," *Science*, vol. 271, no. 5251, pp. 933–937, 1996.

[2] W. U. Huynh, J. J. Dittmer, and A. P. Alivisatos, "Hybrid nanorod-polymer solar cells," *Science*, vol. 295, no. 5564, pp. 2425–2427, 2002.

[3] H. H. Kung and M. C. Kung, "Nanotechnology: applications and potentials for heterogeneous catalysis," *Catalysis Today*, vol. 97, no. 4, pp. 219–224, 2004.

[4] S. Lindroos, A. Arnold, and M. Leskelä, "Growth of CuS thin films by the successive ionic layer adsorption and reaction method," *Applied Surface Science*, vol. 158, no. 1-2, pp. 75–80, 2000.

[5] J.-S. Chung and H.-J. Sohn, "Electrochemical behaviors of CuS as a cathode material for lithium secondary batteries," *Journal of Power Sources*, vol. 108, no. 1-2, pp. 226–231, 2002.

[6] R. S. Mane and C. D. Lokhande, "Chemical deposition method for metal chalcogenide thin films," *Materials Chemistry and Physics*, vol. 65, no. 1, pp. 1–31, 2000.

[7] Q. Wang, N. An, Y. Bai et al., "High photocatalytic hydrogen production from methanol aqueous solution using the photocatalysts CuS/TiO_2," *International Journal of Hydrogen Energy*, vol. 38, no. 25, pp. 10739–10745, 2013.

[8] Y. Han, Y. Wang, W. Gao et al., "Synthesis of novel CuS with hierarchical structures and its application in lithium-ion batteries," *Powder Technology*, vol. 212, no. 1, pp. 64–68, 2011.

[9] A. Šetkus, A. Galdikas, A. Mironas et al., "Properties of Cu_xS thin film based structures: influence on the sensitivity to ammonia at room temperatures," *Thin Solid Films*, vol. 391, no. 2, pp. 275–281, 2001.

[10] T.-Y. Ding, M.-S. Wang, S.-P. Guo, G.-C. Guo, and J.-S. Huang, "CuS nanoflowers prepared by a polyol route and their photocatalytic property," *Materials Letters*, vol. 62, no. 30, pp. 4529–4531, 2008.

[11] P. Roy and S. K. Srivastava, "Hydrothermal growth of CuS nanowires from Cu-dithiooxamide, a novel single-source precursor," *Crystal Growth & Design*, vol. 6, no. 8, pp. 1921–1926, 2006.

[12] H. Zhang, Y. Q. Zhang, J. X. Yu, and D. Yang, "Phase-selective synthesis and self-assembly of monodisperse copper sulfide nanocrystals," *The Journal of Physical Chemistry C*, vol. 112, no. 35, pp. 13390–13394, 2008.

[13] Y. F. Huang, H. N. Xiao, S. G. Chen, and C. Wang, "Preparation and characterization of CuS hollow spheres," *Ceramics International*, vol. 35, no. 2, pp. 905–907, 2009.

[14] C. Wang, K. Tang, Q. Yang, H. Bin, G. Shen, and Y. Qian, "Synthesis of CuS millimeter-scale tubular crystals," *Chemistry Letters*, vol. 30, no. 6, pp. 494–495, 2001.

[15] Y.-B. Chen, L. Chen, and L.-M. Wu, "Water-induced thermolytic formation of homogeneous core-shell CuS microspheres and their shape retention on desulfurization," *Crystal Growth & Design*, vol. 8, no. 8, pp. 2736–2740, 2008.

[16] P. Roy, K. Mondal, and S. K. Srivastava, "Synthesis of twinned CuS nanorods by a simple wet chemical method," *Crystal Growth & Design*, vol. 8, no. 5, pp. 1530–1534, 2008.

[17] M. Saranya and A. N. Grace, "Hydrothermal synthesis of CuS nanostructures with different morphology," *Journal of Nano Research*, vol. 18-19, pp. 43–51, 2012.

[18] Y. Zhao, F. Xiao, and Q. Jiao, "Hydrothermal synthesis of Ni/Al layered double hydroxide nanorods," *Journal of Nanotechnology*, vol. 2011, Article ID 646409, 6 pages, 2011.

[19] M. Saranya, G. Srishti, S. Iksha et al., "Solvothermal preparation of ZnO/graphene nanocomposites and its photocatalytic properties," *Nanoscience and Nanotechnology Letters*, vol. 5, no. 3, pp. 349–354, 2013.

[20] P. Roy and S. K. Srivastava, "Solvothermal growth of flower-like morphology from nanorods of copper sulfides," *Journal of Nanoscience and Nanotechnology*, vol. 8, no. 3, pp. 1523–1527, 2008.

[21] G. Shen, D. Chen, K. Tang, X. Liu, L. Huang, and Y. Qian, "General synthesis of metal sulfides nanocrystallines via a simple polyol route," *Journal of Solid State Chemistry*, vol. 173, no. 1, pp. 232–235, 2003.

[22] X. Wang, C. Xu, and Z. Zhang, "Synthesis of CuS nanorods by one-step reaction," *Materials Letters*, vol. 60, no. 3, pp. 345–348, 2006.

[23] L. Reijnen, B. Meester, F. De Lange, J. Schoonman, and A. Goossens, "Comparison of Cu_xS films grown by atomic layer deposition and chemical vapor deposition," *Chemistry of Materials*, vol. 17, no. 10, pp. 2724–2728, 2005.

[24] P. Roy and S. K. Srivastava, "Low-temperature synthesis of CuS nanorods by simple wet chemical method," *Materials Letters*, vol. 61, no. 8-9, pp. 1693–1697, 2007.

[25] H. Y. He, "Magnetic properties of $Co_{0.5}Zn_{0.5}Fe_2O_4$ nanoparticles synthesized by a template-assisted hydrothermal method," *Journal of Nanotechnology*, vol. 2011, Article ID 182543, 5 pages, 2011.

[26] A. Phuruangrat, T. Thongtem, and S. Thongtem, "Novel combine sonochemical/solvothermal syntheses, characterization and optical properties of CdS nanorods," *Powder Technology*, vol. 233, pp. 155–160, 2013.

[27] W. J. Lou, M. Chen, X. B. Wang, and W. M. Liu, "Size control of monodisperse copper sulfide faceted nanocrystals and triangular nanoplates," *The Journal of Physical Chemistry C*, vol. 111, no. 27, pp. 9658–9663, 2007.

[28] P. Zhang and L. Gao, "Copper sulfide flakes and nanodisks," *Journal of Materials Chemistry*, vol. 13, no. 8, pp. 2007–2010, 2003.

[29] H. L. Xu, W. Z. Wang, and W. Zhu, "Sonochemical synthesis of crystalline CuS nanoplates via an in situ template route," *Materials Letters*, vol. 60, no. 17-18, pp. 2203–2206, 2006.

[30] K.-J. Wang, G.-D. Li, J.-X. Li, Q. Wang, and J.-S. Chen, "Formation of single-crystalline CuS nanoplates vertically standing on flat substrate," *Crystal Growth & Design*, vol. 7, no. 11, pp. 2265–2267, 2007.

[31] W. Du, X. Qian, M. Xiaodong, Q. Gong, H. Cao, and J. Yin, "Shape-controlled synthesis and self-assembly of hexagonal covellite (CuS) nanoplatelets," *Chemistry*, vol. 13, no. 11, pp. 3241–3247, 2007.

[32] A. Ghezelbash and B. A. Korgel, "Nickel sulfide and copper sulfide nanocrystal synthesis and polymorphism," *Langmuir*, vol. 21, no. 21, pp. 9451–9456, 2005.

[33] A.-M. Qin, Y.-P. Fang, H.-D. Ou, H.-Q. Liu, and C.-Y. Su, "Formation of various morphologies of covellite copper sulfide submicron crystals by a hydrothermal method without surfactant," *Crystal Growth & Design*, vol. 5, no. 3, pp. 855–860, 2005.

[34] W. Liang and M.-H. Whangbo, "Conductivity anisotropy and structural phase transition in covellite CuS," *Solid State Communications*, vol. 85, no. 5, pp. 405–408, 1993.

[35] L. F. Chen, W. Yu, and Y. Li, "Synthesis and characterization of tubular CuS with flower-like wall from a low temperature hydrothermal route," *Powder Technology*, vol. 191, no. 1-2, pp. 52–54, 2009.

[36] H. L. Xu, W. Z. Wang, W. Zhu, and L. Zhou, "Synthesis of octahedral CuS nanocages via a solid-liquid reaction," *Nanotechnology*, vol. 17, no. 15, pp. 3649–3654, 2006.

[37] R. H. Kore, J. S. Kulkarni, and S. K. Haram, "Effect of nonionic surfactants on the kinetics of disproportion of copper sulfide nanoparticles in the aqueous sols," *Chemistry of Materials*, vol. 13, no. 5, pp. 1789–1793, 2001.

[38] C. Yang, H. Fan, Y. Xi, J. Chen, and Z. Li, "Effects of depositing temperatures on structure and optical properties of TiO_2 film deposited by ion beam assisted electron beam evaporation," *Applied Surface Science*, vol. 254, no. 9, pp. 2685–2689, 2008.

[39] L. Z. Pei, J. F. Wang, X. X. Tao et al., "Synthesis of CuS and $Cu_{1.1}Fe_{1.1}S_2$ crystals and their electrochemical properties," *Materials Characterization*, vol. 62, no. 3, pp. 354–359, 2011.